ORIGINAL ARTICLE

Development of Pancreatic Acinar Cell Metaplasia During Gastric Repair in a Rat Duodenal Contents Reflux Model

Yasuhiro Wada[1,2,3] · Ken-ichi Mukaisho[2] · Shunpei Kanai[2] · Takahisa Nakayama[2] · Masahide Fukuda[1] ·
Kazuhiro Mizukami[1] · Tadayoshi Okimoto[1] · Masaaki Kodama[1] · Hiroyuki Sugihara[2] · Kazunari Murakami[1] ·
Ryoji Kushima[3]

Abstract

Background We previously reported the development of pancreatic acinar cell metaplasia (PACM) in the glandular stomach of a duodenal contents reflux model (reflux model).

Aims We aimed to investigate the characteristics and histogenesis of PACM using a reflux model.

Methods A reflux model was created using 8-week-old male Wistar rats, which were killed up to 30 weeks postoperatively. Histological examination was performed to analyze the glandular stomach–jejunal anastomosis. Furthermore, electron microscopic images of PACM samples were compared with pancreatic and gastric glands removed from rats that had not undergone surgery. Immunostaining for α-amylase, HIK1083, TFF2, and Ki-67 was performed, and double fluorescent staining was carried out using antibodies against α-amylase and HIK1083, or α-amylase and TFF2.

Results In all reflux model rats, PACM was observed proximal to the glandular stomach–jejunal anastomosis, surrounded by pseudopyloric metaplasia. The number of chief cells was decreased in the deep part of the gland, where PACM occurred. Electron microscopy showed that PACM cells had greater numbers of rough endoplasmic reticulum tubules than chief cells, and exhibited pancreatic acinar cell morphology. Upon immunochemical staining, the regenerative foveolar epithelium and part of the pseudopyloric glands stained strongly positive for TFF2, whereas PACM cells were only weakly positive. Double fluorescent staining identified early lesions of PACM in the neck, which were double positive for α-amylase and TFF2, but negative for HIK1083.

Conclusions PACM could be induced by duodenal contents reflux. PACM originates from stem cells located in the neck of oxyntic glands during gastric mucosal regeneration.

Keywords Pancreatic acinar cell metaplasia · SPEM · Rat reflux model · Bile acids

Abbreviations

PACM	Pancreatic acinar cell metaplasia
GERD	Gastroesophageal reflux disease
H. pylori	*Helicobacter pylori*
SPEM	Spasmolytic polypeptide-expressing metaplasia
TFF2	Trefoil factor 2
HE	Hematoxylin and eosin

✉ Ken-ichi Mukaisho
mukaisho@belle.shiga-med.ac.jp

1 Department of Gastroenterology, Faculty of Medicine, Oita University, Yufu, Oita, Japan

2 Department of Pathology, Shiga University of Medical Science, Seta-tsukinowa-cho, Otsu, Shiga 520-2192, Japan

3 Division of Diagnostic Pathology, Shiga University of Medical Science Hospital, Otsu, Japan

Introduction

Pancreatic acinar cell metaplasia (PACM) is a type of metaplasia that was initially reported in the early 1990s [1], and is mainly found in the gastric mucosa, along with less frequently occurring intestinal and pseudopyloric metaplasia. PACM resembles pancreatic acinar cells, exocrine cells with basophilic cytoplasm, and eosinophilic coarse granules [1–3]. PACM is composed of pancreatic acinar cell-like cells, as observed in gastric mucosa, and differs from the ectopic pancreas that may contain pancreatic ducts or islets of Langerhans [1, 4]. Immunohistochemical staining is reported to be positive

for lipase, trypsin, chymotrypsin, and α-amylase for PACM [1, 2, 4–8].

PACM may be observed in humans with healthy mucosa and atrophic gastritis [1, 9] but is reported to be more frequently observed in the gastric body of Barrett's epithelium and in autoimmune gastritis [10–12]. Reported incidence rates of PACM were 38.0% in Barrett's epithelium [10], 50.0% in autoimmune gastritis, 6.6% in atrophic gastritis, and 2.7% in normal mucosa [9]. On the other hand, it has been reported that PACM is not associated with symptoms of gastroesophageal reflux disease (GERD), histological findings of esophagitis, or chronic gastritis [12]. Therefore, it has been hypothesized that PACM is not acquired and that "metaplasia" is not a suitable term for PACM [12].

Metaplasia refers to the conversion of one cell type to another [13]. Types of metaplasia that occur in the stomach include intestinal and pseudopyloric metaplasia. In intestinal metaplasia, part of the gastric glands changes to intestinal epithelium and is associated with gastric cancer. It is also associated with the chronic inflammation and atrophy of the gastric mucosa due to *Helicobacter pylori* (*H. pylori*) infection [14]. The pseudopyloric metaplasia is associated with gastric inflammation due to *H. pylori* infection and gastric mucosal damage such as gastric ulcer [15–17]. In humans, pseudopyloric metaplasia, pyloric glands stain MUC6 positive [18–20], whereas in rats it stains positive for HIK1083, a protein expressed in mucous neck cells and pyloric glands [21].

We have previously reported a connection between the onset of gastric and esophageal adenocarcinoma and the bile acids contained in duodenal contents, using various rat duodenal reflux models [22–25]. In one of our reflux models, we earlier reported the development of cardiac-type mucosa in the esophagus following surgical procedures that caused reflux of gastric fluid, including duodenal contents, into the esophagus [25]. We also reported the development of PACM in the glandular stomach in this model [26]. In the present study, we examined the histogenesis of PACM using a rat model, in which all duodenal contents were refluxed into the glandular stomach, similar to the model above. Further, we explored the relationship between PACM and spasmolytic polypeptide-expressing metaplasia (SPEM), which occurs during gastric mucosal regeneration [27, 28] and has been reported to be associated with carcinogenesis [29, 30]. Trefoil factor 2 (TFF2) was used as a SPEM marker, which is expressed in parts of pseudopyloric metaplasia and foveolar epithelium [31], while HIK1083 was used as a marker for pyloric gland-type cells.

Methods

Creation of a Rat Duodenal Contents Reflux Model

As previously reported, we created a duodenal contents reflux model using 12 male Wistar rats weighing approximately 250 g at 8 weeks of age using surgical techniques to allow reflux of duodenal contents into the stomach [22]. The procedure is summarized in Fig. 1. Briefly, an upper midline incision was made and the surgical procedure was performed under general anesthesia with isoflurane (Wako, Osaka, Japan). As in previous reports, the glandular stomach and duodenum were dissected at the oral side of the duodenal papilla and the duodenal stump was left as a blind stump. In addition, the jejunum was resected 2 cm from the ligament of Treitz on the anal side, endo-anastomosis of the oral end of the jejunum to the greater curvature of the glandular stomach was performed, and an operation to anastomose the anal end of the jejunum to the stump of the glandular stomach and the duodenum was performed [22]. Rats that underwent surgery started drinking water 12 h postoperatively, and meals were initiated at 36 h postoperatively. Five rats were killed at 4 weeks postoperatively, two at 8 weeks postoperatively, two at 25 weeks postoperatively, and three at 30 weeks postoperatively. In addition, five 25-week-old rats that had not undergone surgery were killed as controls.
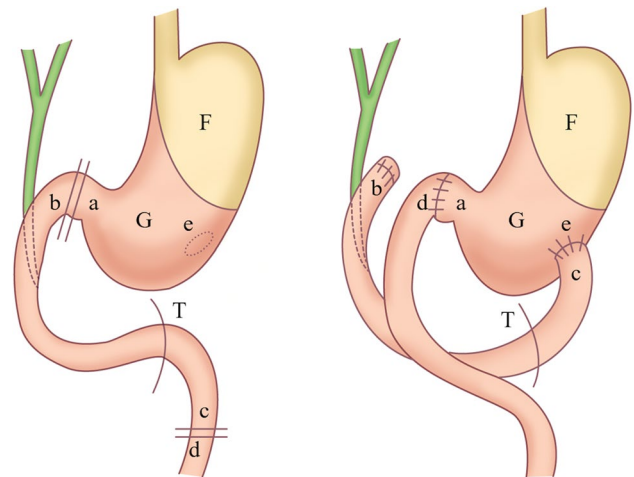

Fig. 1 Rat duodenal reflux model. A preoperative image is shown on the left, while the right half illustrates the surgically induced rat duodenal contents reflux model used in this study. Resection was performed on structures highlighted by double lines, making a blind stump (**b**). Anastomosis was performed between (**a**) and (**d**), as well as (**c**) and (**e**). T, ligament of Treitz; F, forestomach; G, glandular stomach

Histological Examination

The stomach, including the glandular stomach–jejunal anastomosis, was excised from the killed animals, and both, the stomach and pancreas, were excised from the control rats. Excised tissues were fixed in 10% buffered formalin for 24 h. After a paraffin block, fixed tissues were sliced into 2 μm sections and histologically examined following hematoxylin and eosin (HE) staining.

Electron Microscopy

Electron microscopy was performed by Tokai Electron Microscopy, Inc. (Nagoya, Japan). Tissue samples of approximately 2 mm^3 were resected from the vicinity of the glandular stomach–jejunal anastomosis, a site of frequent localization of PACM, from rats 25 weeks postoperatively, while tissues of the glandular stomach mucosa and pancreas were resected from the control rats at 25 weeks of age. The cells were permeabilized and fixed in 2% paraformaldehyde and 2% glutaraldehyde. After washing, cells were fixed with 2% osmium tetroxide followed by dehydration with alcohol. Infiltration with propylene oxide and resin embedding (Quetol-812; Nisshin EM Co., Tokyo, Japan) were performed. The slices were further cut into 1.5 μm sections with a glass knife and stained with 0.5% toluidine blue. Ultra-thin slicing was performed at a thickness of 70 nm using a diamond knife. The primary staining was performed with 2% uranyl acetate and the secondary staining was performed with a lead stain solution (Sigma-Aldrich Co., Tokyo, Japan). Stained sections were observed using a transmission electron microscope (JEM-1400Plus; JOEL Ltd., Tokyo, Japan), and digital images were acquired using a CCD camera (3296 × 2472 pixels, EM-14830RUBY2; JEOL Ltd., Tokyo, Japan).

Immunohistochemical Staining

Immunohistochemical staining was performed using antibodies against α-amylase, HIK1083, TFF2, and Ki-67. The following primary antibodies were used: anti-α-amylase to stain pancreatic acinar cells (dilution ratio: 1:1000; Cell Signaling technology, Danvers, USA, cat.#3796S), anti-HIK1083 for staining pyloric mucous cells (dilution ratio: 1:10; Kanto Kagaku, Tokyo, Japan, cat.#908G1659), anti-TFF2 as a marker for SPEM (dilution ratio: 1:100; Abcam, Cambridge, England, cat.#ab239488), and anti-Ki-67 as a marker for cell proliferation (dilution ratio: 1:100; Abcam, Cambridge, England, cat.#ab16667). An automated device was used for immunohistochemical staining (Ventana Discovery XT, Roche Diagnostics K.K., Tokyo, Japan).

Fluorescence Staining

The gastric mucosa isolated from the animals of the reflux model was fluorescently stained for a combination of either α-amylase and TFF2, or α-amylase and HIK1083. The gastric mucosa and pancreas derived from the control animals were fluorescently stained for TFF2. Primary antibodies used have been listed in the immunohistochemical staining protocol. Alexa Fluor 488 goat anti-rabbit IgG (dilution ratio: 1:200; Invitrogen, Carlsbad, USA, cat.#1212189) and Alexa Fluor 594 goat anti-mouse IgG (dilution ratio: 1:200; Invitrogen, Carlsbad, USA, cat.#1985396) were used as the secondary antibodies, and DAPI (dilution ratio: 1:1000; Wako, Osaka, Japan, cat.#STQ7716) was used for the nuclear staining. The staining was observed using an automated immunohistochemical staining device (Ventana; Discovery XT, Roche Diagnostics K.K., Tokyo, Japan).

Results

Histological Examination of PACM

Our results showed that PACM occurred near the glandular stomach–jejunal anastomosis in all animals of reflux model. The PACM cells were sporadically distributed from the neck to the bottom of the oxyntic glands (Fig. 2a, b) and were positive for α-amylase (Fig. 2c). Proliferating cells positive for Ki-67 were more common in the neck of gastric oxyntic glands, but infrequent in small lesions of PACM (Fig. 2d). Interestingly, large aggregates of α-amylase-positive PACM cells with a budding and sac-like appearance (Fig. 2e–g), which were developed in the deeper parts of the oxyntic glands, showed slightly higher Ki-67 indices (Fig. 2h).

Electron Microscopy Images

As shown by toluidine blue staining, PACM cells located around the neck of the oxyntic gland resembled a normal oxyntic gland with simple tubular gland morphology (Fig. 3a). However, PACM near the bottom of the oxyntic gland showed acinar structure, similar to a normal exocrine pancreas. Many zymogen granules were observed in the apical cytoplasm of cells present in PACM (Fig. 3b). The PACM cells were larger than chief cells (Fig. 3c) and had a higher resemblance to pancreatic acinar cells (Fig. 3d) than to chief cells (Fig. 3b–d). Moreover, the rough endoplasmic reticulum was more developed in PACM and pancreatic acinar cells than in chief cells (Fig. 3b–d).
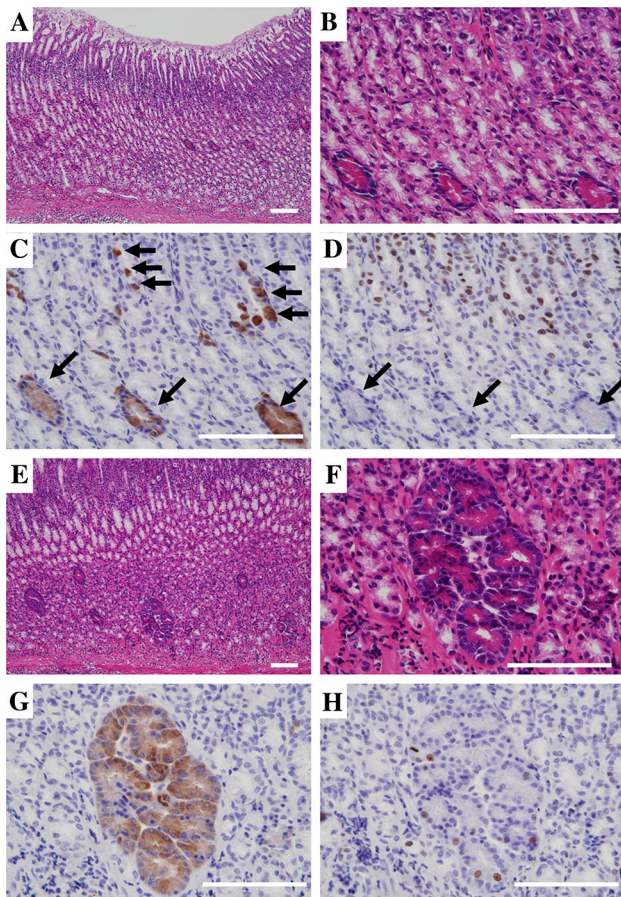
Fig. 2 Hematoxylin and eosin (HE) staining and immunohistochemical staining of α-amylase and Ki-67 in pancreatic acinar cell metaplasia. Tissue slices of pancreatic acinar cell metaplasia (PACM) derived from reflux model rats 4 weeks postoperatively were subjected to staining with hematoxylin and eosin (HE) (**a**, **b**, **e**, **f**), and antibodies against α-amylase (**c**, **g**) or Ki-67 (**d**, **h**). Arrows indicate small lesions of PACM. Each scale bar represents 200 μm

Fig. 3 Toluidine blue staining and electron microscopy imaging. PACM from the reflux model 25 weeks postoperatively was stained with toluidine blue on 1.5 μm thin sections derived from regions surrounding the glandular stomach–jejunal anastomosis (**a**). Ultra-thin slices of reflux model PACM (**b**), chief cells (**c**), and pancreatic acinar cells (**d**) were contrasted with 2% uranyl acetate and a lead stain solution. Each scale bar represents 200 μm in **a** and 5 μm in **b**–**d**

Association Between PACM and SPEM

TFF2-positive cells were partly seen in the gastric oxyntic mucosa far from the anastomotic site of reflux model animals (Fig. 4a). In the pancreas, acinar cells but not islet cells of Langerhans were positive for TFF2 (Fig. 4b). The PACM was detected in the gastric oxyntic mucosa derived from reflux model animals (Fig. 4c). Strong TFF2 staining was observed in foveolar epithelial cells with regenerative changes, while PACM cells stained weakly (Fig. 4d). Further, pseudopyloric metaplasia cells with a bright cytoplasm were observed around PACM (Fig. 4c). The pseudopyloric metaplasia tested positive for HIK1083 (Fig. 4e). In the deeper part of the gland, where PACM and pseudopyloric glands were located, chief cells either decreased in number or completely disappeared (Fig. 4f). PACM was not observed in the glandular stomach in control rats. No neoplasms, such
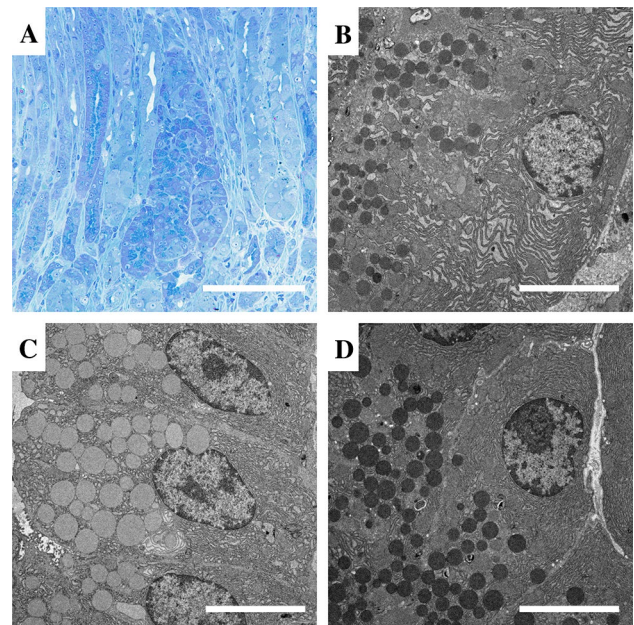
as dysplasia or cancer, were observed in any of the animals of reflux models during the study period.

Double Fluorescent Staining

Intense TFF2 immunoreactivity was observed in regenerative gastric foveolar epithelium and accessory cells in the luminal side of PACM, whereas cells of the PACM proper showed comparably weaker immunoreactivity (Fig. 5a, b). All PACM cells stained positive for α-amylase (Figs. 5c, 6c), and pseudopyloric metaplasia around PACM was positive for HIK1083 (Fig. 6b). Fluorescence signals of TFF2 and α-amylase overlapped in PACM cells (Fig. 5d), but colocalization of α-amylase and HIK1083 was not observed by double fluorescent staining (Fig. 6d).

Discussion

PACM was observed near the glandular stomach–jejunal anastomosis in all reflux model rats 4 weeks postoperatively. It was distributed from the neck to the bottom of the oxyntic gland. TFF2 was weakly expressed in PACM. Electron microscopy revealed that PACM cells formed a tubular gland, similar to the oxyntic gland, in the neck part of the gastric mucosa. These results suggested that PACM cells
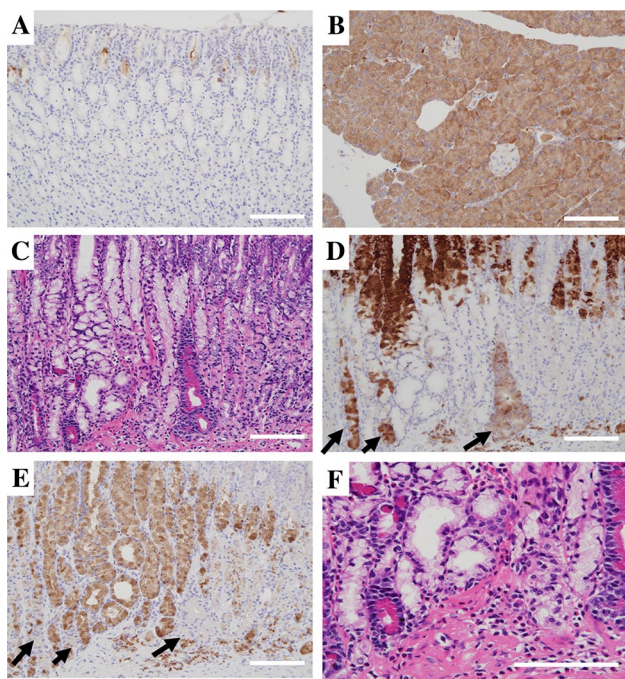
Fig. 4 Immunostaining of pancreatic acinar cell metaplasia developed in duodenal content reflux model. Gastric oxyntic mucosa far from the anastomotic site of the reflux model 25 weeks postoperatively (**a**) and pancreas tissue of the control rats (**b**) were stained with TFF2. Tissue slices of PACM derived from the reflux model were subjected to staining with HE (**c**), TFF2 (**d**) and HIK1083 (**e**). HE staining of the deeper part of the gland (**f**). Arrows indicate PACM. Each scale bar represents 200 μm

Fig. 5 Double fluorescent staining of TFF2 and α-amylase. Tissue slices were stained with HE (**a**), and antibodies against TFF2 (red) (**b**), or α-amylase (green) (**c**). A composite image of TFF2 and α-amylase staining is shown in (**d**). Nuclei were stained with DAPI (blue). Each scale bar represents 200 μm

probably originate from stem cells present in the neck of the oxyntic gland during regeneration after mucosal injury caused by duodenal contents reflux [32, 33]. In the deeper part of the oxyntic gland, PACM showed a budding, sac-like appearance, and a higher Ki-67 index compared to the smaller PACM lesions located at the neck. These findings suggested that the smaller PACM lesions in the neck region probably migrate downward, enhance proliferative activity, and develop budding acinar structures.

The precise molecular mechanism underlying the development of PACM remains unknown. Because PACM is observed in children without inflammation or intestinal metaplasia [4, 12, 34], it may be a remnant of the fetal period and has been reported to be congenital [5]. However, our results from this study suggest that at least some cases of PACM could be acquired. In the present study, pseudopyloric metaplasia, which consists of pyloric-type mucous glands, was present in the background of PACM. In human cases, cardiac-type mucosa is often observed surrounding PACM [1, 8]. Moreover, PACM could be considered an aberrant differentiation phenotype of chief cell precursors as there is some ultrastructural resemblance between gastric chief cells and pancreatic acinar cells [8]. Mucous neck cells
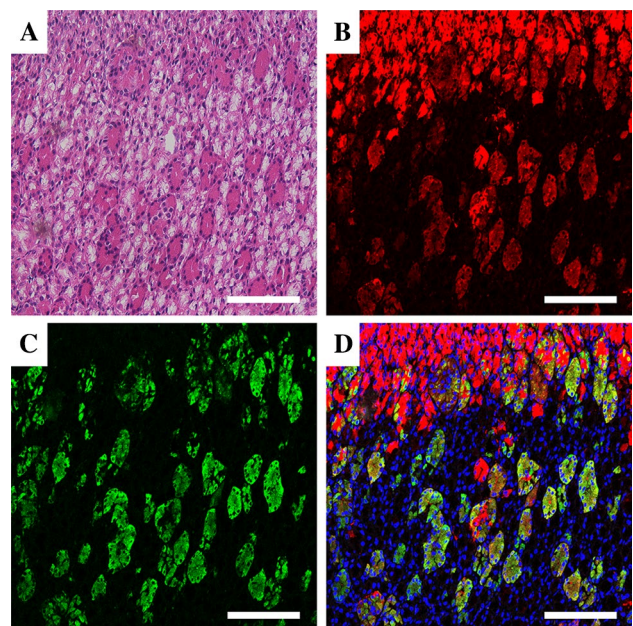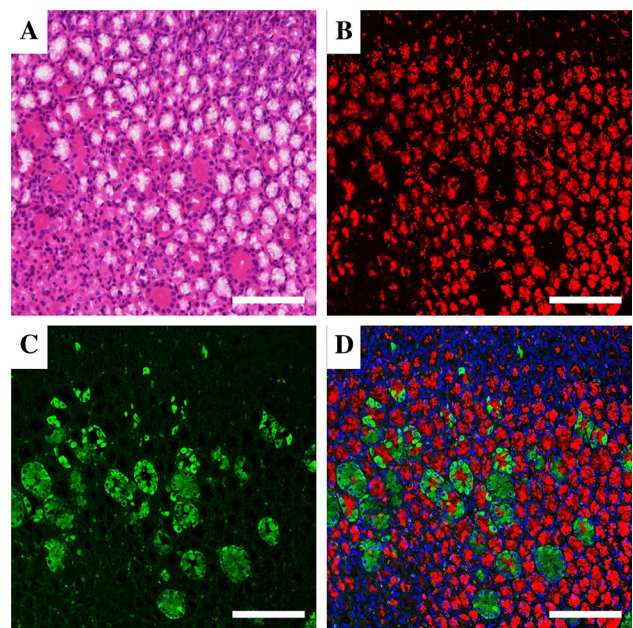

Fig. 6 Double fluorescent staining of HIK1083 and α-amylase. Tissue slices were stained with HE (**a**), or antibodies against HIK1083 (red) (**b**), and α-amylase (green) (**c**). A composite image of HIK1083 and α-amylase staining is shown in (**d**). Nuclei were stained with DAPI (blue). Each scale bar represents 200 μm

are reported to be the precursors of chief cells [26]. Since the PACM cells, as well as mucous neck cells, were positive for TFF2 in the regenerative mucosa in the animals of reflux model, and because the expression pattern of a mucous neck cell marker (HIK1083) and a PACM marker (α-amylase) did not overlap, we hypothesize that the TFF2-positive, regenerative cells could differentiate bidirectionally into PACM and pseudopyloric metaplasia.

In 1999, Schmidt et al. reported that TFF2 was expressed in metaplastic cells adjacent to the gastric cancer in the stomach [35]. This was the first study to report the TFF2- and MUC6-positive pyloric gland in SPEM [36]. SPEM occurs during the acute damage to the gastric mucosa and gastric ulceration caused by drugs such as DMP777, L635, or high-dose tamoxifen in addition to *H. pylori* infection [29, 37, 38] and plays a role in regeneration in response to gastric mucosal injury [29, 39, 40]. While SPEM associated with acute gastric mucosal injury contributes to gastric mucosal regeneration, the continued presence of SPEM in chronic inflammatory conditions may lead to gastric cancer [30]. Kaise et al. reported that TFF2 was predominantly expressed in regenerative foveolar epithelium and partially in the pyloric glands in 18 gastric ulcer patients [31]. In the present study, TFF2 was also expressed in the foveolar epithelium of the gastric mucosa near the glandular stomach–jejunal anastomosis and in some pyloric-type gland cells around PACM. These pyloric-type gland cells positive for TFF2 appear to correspond to SPEM. However, because fluorescence signals of HIK1083 and TFF2 did not completely co-localized, SPEM and pseudopyloric metaplasia are not the same lesions in the strict sense.

In the present study, PACM was induced by the reflux of duodenal juices into the glandular stomach of rats. Earlier, we succeeded in inducing PACM by long-term administration of proton pump inhibitors (PPI), as well as in the reflux model [41]. Furthermore, the study compared the incidence of PACM between a placebo group and a PPI-treated group, using a rat reflux model of the esophagogastric junction, showing that the occurrence of PACM significantly increased in the PPI-treated group [42]. In humans, PACM is observed in cases of autoimmune and atrophic gastritis [9]. These results suggest that a low acid content in stomach may be related to the development of PACM. The duodenal reflux contains bile juice, which in humans contains approximately 60% glycine-conjugated bile acid with an acid dissociation coefficient (pKa) ranging from 4 to 5, approximately 20% taurine-conjugated bile acids with a pKa of approximately 2, and the unconjugated bile acids [43, 44]. Even in healthy subjects, duodenal contents flow back into the stomach after eating, but the pH in the stomach is approximately 2, and the acids other than taurine-conjugated bile acids precipitate. Moreover, glycine-conjugated bile acids do not precipitate under mild acidic conditions (pH > 4). The bile acid

concentrations in gastric juice are approximately four times greater than under pH > 4 [43, 44]. It has been reported that in humans, the bile acid concentrations increased in gastric juice in response to PPI administration [45]. Since the esophagogastric junction is located on the dorsal side of the body, when a person lies down in the supine position immediately after eating, the esophagogastric junction is exposed to bile acid reflux. Since bile acids are involved in the onset of Barrett's esophagus [24, 46–48] and PACM too is suggested to be associated with Barrett's esophagus, bile acids may be associated with PACM.

In conclusion, our results suggested that at least some of the cases of PACM could be acquired. Further, some cases of PACM were associated with the gastric mucosal damage due to the reflux of duodenal contents containing bile acids. In addition, PACM and pseudopyloric metaplasia might originate from stem cells in the neck of the oxyntic glands. However, since fluorescence signals of HIK1083 and α-amylase did not co-localize, we hypothesize that upon regeneration of gastric mucosa, the stem cells of the neck may differentiate bidirectionally into PACM and pseudopyloric metaplastic lineages.

Compliance with Ethical Standards

Conflict of interest The authors declare that they have no conflict of interest.

Ethical approval All experiments were conducted in accordance with the guidelines for animal experiments at the Research Center for Animal Life Science of the Shiga Medical University, in accordance with the ethical rules regarding the use of experimental animals (Experiment Approval Number: 2018-1-2).

References

1. Doglioni C, Laurino L, Dei Tos AP, et al. Pancreatic (acinar) metaplasia of the gastric mucosa. Histology, ultrastructure, immunocytochemistry, and clinicopathologic correlations of 101 cases. *Am J Surg Pathol*. 1993;17:1134–1143.

2. Krishnamurthy S, Dayal Y. Pancreatic metaplasia in Barrett's esophagus. An immunohistochemical study. *Am J Surg Pathol*. 1995;19:1172–1180.

3. Stachura J, Konturek JW, Urbanczyk K, et al. Endoscopic and histological appearance of pancreatic metaplasia in the human gastric mucosa: a preliminary report on a recently recognized new type of gastric mucosal metaplasia. *Eur J Gastroenterol Hepatol*. 1996;8:239–243.

4. Integlia MJ, Krishnamurthy S, Berhane R, et al. Pancreatic metaplasia of the gastric mucosa in pediatric patients. *Am J Gastroenterol*. 1997;92:1553–1556.

5. Wang HH, Zeroogian JM, Spechler SJ, et al. Prevalence and significance of pancreatic acinar metaplasia at the gastroesophageal junction. *Am J Surg Pathol*. 1996;20:1507–1510.

6. Ambrosini-Spaltro A, Potì O, De Palma M, et al. Pancreatic-type acinar cell carcinoma of the stomach beneath a focus of pancreatic metaplasia of the gastric mucosa. *Hum Pathol*. 2009;40:746–749.

7. Håkansson HO, Mellblom L, Johansson J, et al. Synthesis and localization of pancreatic secretory proteins in pancreatic acinar-like metaplasia in the distal part of the oesophagus. Pancreatic acinar metaplasia: another source of pancreatic enzymes! *Scand J Gastroenterol*. 2003;38:10–13.

8. Stachura J, Konturek J, Urbańczyk K, et al. Pancreatic metaplasia of the human gastric mucosa is associated with high expression of transforming growth factor alpha but not of epidermal growth factor. *Histopathology*. 1995;27:509–515.

9. Jhala NC, Montemor M, Jhala D, et al. Pancreatic acinar cell metaplasia in autoimmune gastritis. *Arch Pathol Lab Med*. 2003;127:854–857.

10. Johansson J, Håkansson HO, Mellblom L, et al. Pancreatic acinar metaplasia in the distal oesophagus and the gastric cardia: prevalence, predictors and relation to GORD. *J Gastroenterol*. 2010;45:291–299.

11. Chlumská A, Boudová L, Benes Z, et al. Autoimmune gastritis. A clinicopathologic study of 25 cases. *Cesk Patol*. 2005;41:137–142.

12. Schneider NI, Plieschnegger W, Geppert M, et al. Pancreatic acinar cells—a normal finding at the gastroesophageal junction? Data from a prospective Central European multicenter study. *Virchows Arch*. 2013;463:643–650.

13. Thowfeequ S, Myatt EJ, Tosh D. Transdifferentiation in developmental biology, disease, and in therapy. *Dev Dyn*. 2007;236:3208–3217.

14. IARC. Infection with *Helicobacter pylori*. *Monogr Eval Carcinog Risks Hum*. 1994;61:177–240.

15. Xia HH-X, Yang Y, Lam SK, et al. Aberrant epithelial expression of trefoil family factor 2 and mucin 6 in *Helicobacter pylori* infected gastric antrum, incisura, and body and its association with antralisation. *J Clin Pathol*. 2004;57:861–866.

16. Graham DY. History of *Helicobacter pylori*, duodenal ulcer, gastric ulcer, and gastric cancer. *World J Gastroenterol*. 2014;20:5191–5204.

17. Fox JG, Rogers AB, Whary MT. Accelerated progression of gastritis to dysplasia in the pyloric antrum of TFF2 –/– C57BL6 x Sv 129 Helicobacter pylori-infected mice. *Am J Pathol*. 2007;171:1520–1528.

18. Fiocca R, Villani L, Tenti P, et al. Characterization of four main cell types in gastric cancer: foveolar, mucopeptic, intestinal columnar and goblet cells. An histopathologic, histochemical and ultrastructural study of early and advanced tumors. *Pathol Res Pract*. 1987;182:308–325.

19. Ho SB, Roberton AM, Shekels LL, et al. Expression cloning of gastric mucin complementary DNA and localization of mucin gene expression. *Gastroenterology*. 1995;109:735–747.

20. De Bolos C, Garrido M, Real FX. MUC6 apomucin shows a distinct normal tissue distribution that correlates with Lewis antigen expression in the human stomach. *Gastroenterology*. 1995;190:723–734.

21. Ishihara K, Kurihara M, Goso Y, et al. Peripheral alpha-linked N-acetylglucosamine on the carbohydrate moiety of mucin derived from mammalian gastric gland mucous cells: epitope recognized by a newly characterized monoclonal antibody. *Biochem J*. 1996;318:409–416.

22. Mukaisho K, Miwa K, Kumagai H, et al. Gastric carcinogenesis by duodenal reflux through gut regenerative cell lineage. *Dig Dis Sci*. 2003;48:2153–2158. https://doi.org/10.1023/B:DDAS.00000 04519.26201.a4.

23. Kumagai H, Mukaisho K, Sugihara H, et al. Thioproline inhibits development of esophageal adenocarcinoma induced by gastroduodenal reflux in rats. *Carcinogenesis*. 2004;25:723–727.

24. Mukaisho K, Kanai S, Kushima R, et al. Barretts's carcinogenesis. *Pathol Int*. 2019;69:319–330.

25. Kushima R, Mukaisho K, Takemura S, et al. Barrett's esophagus: analyses from human and experimental animal studies. *Pathologe*. 2013;34:138–147. **(in German)**.

26. Mukaisho K. Relationship between development of pancreatic acinar cell metaplasia and duodenal contents reflux: analyses from experimental animal studies. *Ther Res*. 2014;35:387–392.

27. Tran CP, Cook GA, Yeomans ND, et al. Trefoil peptide TFF2 (spasmolytic polypeptide) potently accelerates healing and reduces inflammation in a rat model of colitis. *Gut*. 1999;44:636–642.

28. Cook GA, Familari M, Thim L, et al. The trefoil peptides TFF2 and TFF3 are expressed in rat lymphoid tissues and participate in the immune response. *FEBS Lett*. 1999;456:155–159.

29. Nomura S, Yamaguchi H, Ogawa M, et al. Alterations in gastric mucosal lineages induced by acute oxyntic atrophy in wild-type and gastrin-deficient mice. *Am J Physiol Gastrointest Liver Physiol*. 2005;288:G362–G375.

30. Goldenring JR. Pyloric metaplasia, pseudopyloric metaplasia, ulcer-associated cell lineage and spasmolytic polypeptide-expressing metaplasia: reparative lineages in the gastrointestinal mucosa. *J Pathol*. 2018;245:132–137.

31. Kaise M, Miwa J, Fujimoto A, et al. Influence of *Helicobacter pylori* status and eradication on the serum levels of trefoil factors and pepsinogen test: serum trefoil factor 3 is a stable biomarker. *Gastric Cancer*. 2013;16:329–337.

32. Hattori T, Fujita S. Tritiated thymidine autoradiographic study on cellular migration in the gastric gland of the golden hamster. *Cell Tissue Res*. 1976;172:171–184.

33. Barker N, Huch M, Kujala P, et al. Lgr5(+ve) stem cells drive self-renewal in the stomach and build long-lived gastric units in vitro. *Cell Stem Cell*. 2010;6:25–36.

34. Krishnamurthy S, Integlia MJ, Grand RJ, et al. Pancreatic acinar cell clusters in pediatric gastric mucosa. *Am J Surg Pathol*. 1998;22:100–105.

35. Schmidt PH, Lee JR, Joshi V, et al. Identification of a metaplastic cell lineage associated with human gastric adenocarcinoma. *Lab Invest*. 1999;79:639–646.

36. Lennerz JK, Kim SH, Oates EL, et al. The transcription factor MIST1 is a novel human gastric chief cell marker whose expression is lost in metaplasia, dysplasia and carcinoma. *Am J Pathol*. 2010;177:1514–1533.

37. Bertaux-Skeirik N, Wunderlich M, Teal E, et al. CD44 variant isoform 9 emerges in response to injury and

contributes to the regeneration of the gastric epithelium. *J Pathol*. 2017;242:463–475.

38. Goldenring JR, Gregory S, Ray Robert J, et al. Reversible drug-induced oxyntic atrophy in rats. *Gastroenterology*. 2000;118:1080–1093.

39. Nam KT, Lee HJ, Sousa JF, et al. Mature chief cells are cryptic progenitors for metaplasia in the stomach. *Gastroenterology*. 2010;139:2028–2037.

40. Huh WJ, Khurana SS, Geahlen JH, et al. Tamoxifen induces rapid, reversible atrophy, and metaplasia in mouse stomach. *Gastroenterology*. 2012;142:21–24.

41. Hagiwara T, Mukaisho K, Ling ZQ, et al. Development of pancreatic acinar cell metaplasia after successful administration of omeprazole for 6 months in rats. *Dig Dis Sci*. 2007;52:1219–1224. https://doi.org/10.1007/s10620-006-9253-7.

42. Dall'Olmo L, Fassan M, Dassie E, et al. Role of proton pump inhibitor on esophageal carcinogenesis and pancreatic acinar cell metaplasia development: an experimental in vivo study. *PLoS ONE*. 2014;9:e112862.

43. Mukaisho K, Hagiwara T, Nakayama T, et al. Potential mechanism of corpus-predominant gastritis after PPI therapy in *Helicobacter pylori*-positive patients with GERD. *World J Gastroenterol*. 2014;20:11962–11965.

44. Stamp DH. Three hypotheses linking bile to carcinogenesis in the gastrointestinal tract: certain bile salts have properties that may be used to complement chemotherapy. *Med Hypotheses*. 2002;59:398–405.

45. Foltz E, Azad S, Everett ML, et al. An assessment of human gastric fluid composition as a function of PPI usage. *Physiol Rep*. 2015;3:e12269.

46. Nehra D, Howell P, Williams CP, et al. Toxic bile acids in gastro-oesophageal reflux disease: influence of gastric acidity. *Gut*. 1999;44:598–602.

47. Sun D, Wang X, Gai Z, et al. Bile acids but not acidic acids induce Barrett's esophagus. *Int J Clin Exp Pathol.*. 2015;8:1384–1392.

48. Stein HJ, Barlow AP, DeMeester TR, et al. Complications of gastroesophageal reflux disease. Role of the lower esophageal sphincter, esophageal acid and acid/alkaline exposure, and duodenogastric reflux. *Ann Surg*. 1992;216:35–43.